

Proceedings Article

# Limitations of current MPI models in the context of fluid dynamics

Martin Möddel <sup>a,b,\*</sup> · Anja Schlömerkemper<sup>c</sup> · Tobias Knopp <sup>a,b</sup> · Tobias Kluth <sup>d</sup>

<sup>a</sup>Section for Biomedical Imaging, University Medical Center Hamburg-Eppendorf, Hamburg, Germany

<sup>b</sup>Institute for Biomedical Imaging, Hamburg University of Technology, Hamburg, Germany

<sup>c</sup>Institute of Mathematics, University of Würzburg, Würzburg, Germany

<sup>d</sup>Center for Industrial Mathematics, University of Bremen, Bremen, Germany

\*Corresponding author, email: [m.hofmann@uke.de](mailto:m.hofmann@uke.de)

© 2023 Möddel *et al.*; licensee Infinite Science Publishing GmbH

This is an Open Access article distributed under the terms of the Creative Commons Attribution License (<http://creativecommons.org/licenses/by/4.0>), which permits unrestricted use, distribution, and reproduction in any medium, provided the original work is properly cited.

## Abstract

Micromagnetic fluids are at the core of magnetic particle imaging as underlying tracer materials. They are formed when magnetic nanoparticles are suspended in a fluid such as blood, cytoplasm or water. One of the fundamental assumptions made in current MPI models is that the micromagnetic response of nanoparticles and the dynamics of the fluid transporting them are decoupled. In this contribution, we use a simplified micromagnetic model that takes this interaction into account to investigate scenarios where this assumption breaks down.

## 1. Introduction

Magnetic particle imaging (MPI) is a tracer based tomographic imaging modality, which relies on the nonlinear magnetization response of a tracer material to a dynamic magnetic field for imaging its spatial distribution [1]. These tracer materials are typically nanosized ferrimagnetic iron oxide particles suspended in a fluid such as blood, cytoplasm or water, which then are also referred to as micromagnetic fluids [2]. As one of the key levers for improving MPI's imaging performance, ongoing efforts are being made to optimize these tracers for specific imaging systems and applications [3–5]. What makes MPI particularly interesting from a medical point of view is the high temporal resolution that can be achieved [6, 7], with volumes with a size of about 4 cm<sup>3</sup> scanned in only 21.5 ms [8]. Possible applications are the visualization of instruments for cardiovascular intervention [7, 9–11], real-time perfusion imaging in acute stroke [12–14], magnetic fluid hyperthermia treatment [15], or 3D blood flow quantification [16].

A fundamental limitation for applications of this type

is that the MPI imaging equation was originally formulated for imaging scenarios in which the spatial distribution of the tracer during the acquisition of an image is assumed to be static to a good approximation [17, 18]. If this assumption is violated, more or less noticeable motion artifacts occur [19]. To address this problem, recent generalizations of the imaging equation do take dynamic tracer distributions into account [20, 21] and several approaches for their reconstruction have been proposed [19–24]. An important detail is that the aforementioned MPI models deal with spatiotemporal variations of the tracer that occur at the macroscopic level, i.e., changes in its spatial distribution.

In this work we consider a scenario where the MPI tracer is dispersed in a fluid whose spatiotemporal variations is described by fluid dynamics. This allows to investigate the limits of the aforementioned macroscopic description, where micromagnetic response of nanoparticles and the dynamics of the fluid transporting them are decoupled. A similarly fundamental question about the linearity of dynamic magnetic behavior of a tracer for high tracer concentrations [25] has been studied by mi-

romagnetic models, which could attribute this to magnetic dipole-dipole interactions [26]. As there is no general mathematical MPI model covering the scenario considered here, we use a simplified micromagnetic model to obtain the magnetization response of tracer particles moving along a dynamic fluid in our study.

## II. Problem statement

To illustrate the problem, we consider the scenario where an MPI tracer is uniformly distributed along a circle in the  $xy$ -plane centered around the field free point (FFP) of an ideal MPI selection field. Without any additional excitation field the magnetization of the tracer aligns with the selection field. If we now assume that the particles move in unison along the fluid at a constant speed along the circle, this motion leaves the macroscopic tracer distribution unchanged. However, if we follow the tracer particles along their trajectory, these move through a varying magnetic field. In case the alignment of the magnetic moments with the magnetic field is instantaneous, the magnetization along the circle will remain determined by the local field. If we, however, consider non-instantaneous relaxation dynamics, this will no longer be the case. Instead the local magnetization along the circle will also depend on the “magnetic history” of the particles and hence on the dynamics of the carrier fluid.

## III. Methods

In this contribution we use a simplified Brownian relaxation model [27] without thermal fluctuations. The dynamics of the magnetic moment  $\mathbf{m} : [0, +\infty) \rightarrow \mathbb{S}^2$  of a nanoparticle is determined by the following equation

$$\frac{d\mathbf{m}}{dt} = \frac{(\mathbf{m} \times \boldsymbol{\xi}) \times \mathbf{m}}{2\tau_B}, \quad (1)$$

where  $\tau_B = \frac{3\eta V_h}{kT}$  is the Brownian relaxation time with the suspension viscosity  $\eta$ ,  $V_h$  is the hydrodynamic volume of the particle,  $k$  is the Boltzmann's constant,  $T$  is the temperature, and  $\boldsymbol{\xi} = \frac{\mu\mathbf{H}}{kT}$  with the magnetic moment  $\mu = M_s V_c$ , which is calculated using the material-dependent saturation magnetization  $M_s$  and the core volume  $V_c$ . We assume monodisperse spherical nanoparticles with magnetite core ( $M_s = 420 \text{ kAm}^{-1}$ ) with a diameter of 25 nm resulting in  $\mu = 3.4 \times 10^{-18} \text{ Am}^{-2}$ . For the remaining parameters we consider a temperature of  $T = 293 \text{ K}$  and the following scenarios: (a) nanoparticles with a small hydrodynamic diameter of 75 nm are suspended in water ( $\eta \approx 1 \times 10^{-3} \text{ Pas}$  [28]), (b) nanoparticles with a large hydrodynamic diameter of 250 nm are suspended in blood ( $\eta \approx 3.26 \times 10^{-3} \text{ Pas}$  [29]). Solutions are approximated numerically.

As for the remaining setting we expand on the scenario described above and consider a micromagnetic

fluid as MPI tracer, which is uniformly distributed along a circle of  $r = 5 \text{ cm}$  radius, a selection field  $\mathbf{H}_s(\mathbf{r}) = \mathbf{G}\mathbf{r}$  with a gradient strength of  $\mathbf{G} = \text{diag}(-1, -1, 2) \text{ T m}^{-1}$ , and a sinusoidal excitation field  $\mathbf{H}_{\text{DF}}(t) = (0, 0, A_{\text{DF}} \sin(2\pi f_{\text{DF}} t))$  with  $A_{\text{DF}} = 20 \text{ mT}$  and  $f_{\text{DF}} = 1 \text{ kHz}$ . Next, we distinguish two scenarios: (i) the nanoparticles move in unison along the fluid at a constant speed clockwise on the circle with a given frequency  $f$ , (ii) in the static scenario there is no fluid motion and the nanoparticles remain at their position on the circle. In case (i) the trajectories of the nanoparticles are described by

$$\boldsymbol{\gamma}_b(t) = (r \sin(2\pi(f t + b)), r \cos(2\pi(f t + b)), 0), \quad (2)$$

where  $b \in [0, 1)$  parameterizes the initial position  $\boldsymbol{\gamma}_b(0)$  on the circle at time  $t = 0$ .

For both scenarios we are interested in the signal of the magnetic moment for all locations on the circle  $\mathbf{r}_b = \boldsymbol{\gamma}_b(0)$  with  $b \in [0, 1)$ . Now fix an arbitrary  $b \in [0, 1)$ . In scenario (ii) the signal  $\mathbf{m}_{\text{static},b}(t)$  is obtained by solving equation (1) directly with the field sequence  $\mathbf{H}(t) = \mathbf{H}_s(\boldsymbol{\gamma}_b(0)) + \mathbf{H}_{\text{DF}}(t)$  these particles are exposed to. In scenario (i), we change the frame of reference to the moving particle moving along  $\boldsymbol{\gamma}_b$  to obtain the magnetic moment  $\mathbf{m}_{\text{movref},b}(t)$  by solving equation (1) with the magnetic field sequence  $\mathbf{H}(t) = \mathbf{H}_s(\boldsymbol{\gamma}_b(t)) + \mathbf{H}_{\text{DF}}(t)$  the moving particle is exposed to in this frame of reference. We observe that the magnetic moment  $\mathbf{m}_{\text{motion},b}(t)$  at a fixed location  $\mathbf{r}_b$  and time  $t$  in the original frame of reference is given by the magnetic moment of the particles that happen to pass by at that time

$$\mathbf{m}_{\text{motion},b}(t) = \mathbf{m}_{\text{movref},b-ft}(t) \quad \text{for any } t \in [0, +\infty). \quad (3)$$

## IV. Results

A comparison of the signals  $\mathbf{m}_{\text{static},b}(t)$  and  $\mathbf{m}_{\text{motion},b}(t)$  reveals subtle signal changes in the  $x$ - and  $y$ -component. The direction of the signal difference  $\Delta\mathbf{m}_b = \mathbf{m}_{\text{static},b}(t) - \mathbf{m}_{\text{motion},b}(t)$  depends on the location  $\mathbf{r} = \boldsymbol{\gamma}_b(0)$  and its strength is proportional to the motion frequency  $f$ . Figure 1 shows the signal  $\mathbf{m}_{\text{static},b}(t)$  without fluid motion and the relative signal changes w.r.t. scenario (i) with a motion frequency  $f = 1 \text{ Hz}$  for nanoparticles with a small hydrodynamic diameter suspended in water (a) and nanoparticles with a large hydrodynamic diameter suspended in blood (b). In scenario (i), the particles move with a velocity that is in the range of peak velocities of blood flow in normal human venae cavae of  $0.30 \text{ m s}^{-1}$  to  $0.45 \text{ m s}^{-1}$  [30]. For nanoparticles with small hydrodynamic volume in water (a) one observes a relative deviation up to  $2 \times 10^{-3}$ . For nanoparticles with a large hydrodynamic diameter (b) this error increases by an order of magnitude. Further numerical analysis of our model indicates that these differences are primarily caused by differences in the ratio  $\frac{\xi}{\tau_B}$ .

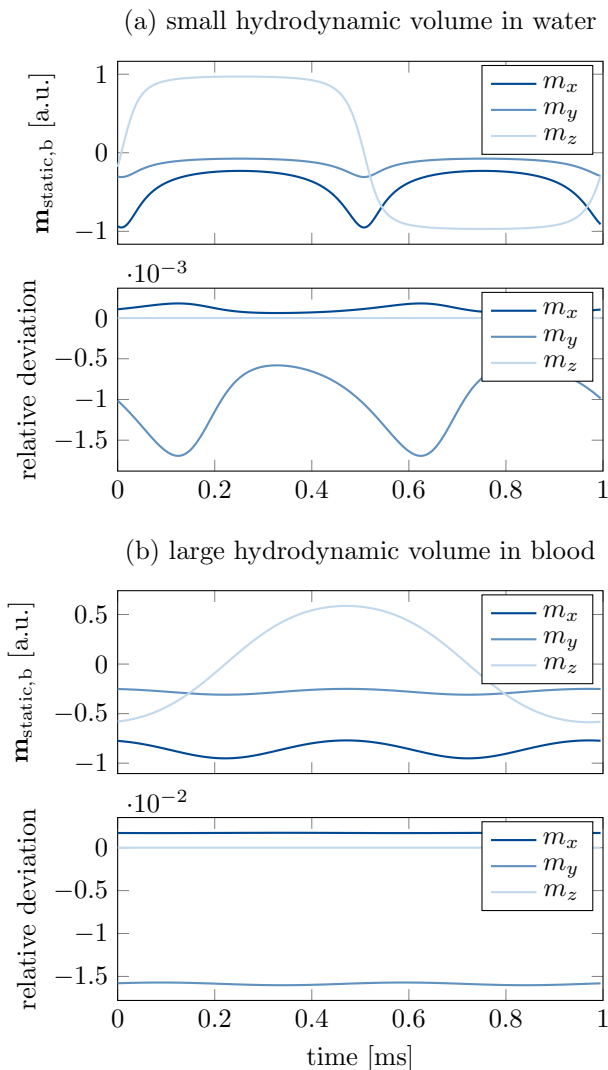


**Figure 1:** The top two graphs show the behavior of the magnetic moment of hydrodynamically small nanoparticles in water (a) and the bottom two show the behavior of hydrodynamically large ones in blood (b), each for  $b = 0.2$  and  $f = 1$  Hz. Top graphs do show the signal for the static setting  $m_{\text{static},b}$ . The relative deviation  $\frac{m_{i,\text{static},b}(t) - m_{i,\text{motion},b}(t)}{m_{i,\text{static},b}(t)}$ ,  $i = x, y, z$  is shown at the bottom, respectively.

## V. Discussion and Conclusion

The subtle signal differences found in our analysis indicate that the coupling between the micromagnetic response of nanoparticles and the dynamics of the fluid transporting, which have not yet found their way into MPI models, have an influence on the local magnetization signals. Our study shows that this influence is negligible for nanoparticles with a small hydrodynamic diameter in water. More generally, we have found that the signal differences are caused by the changes in the magnetic field sequences that drive the magnetization response. Thereby, the strength of the signal changes

depends primarily on the flow velocity of the particles and the ratio  $\frac{\xi}{\tau_B}$ . For nanoparticles with a large hydrodynamic diameter in blood the relative deviation is in the order of one percent. Scenarios where the deviation can no longer be neglected are therefore quite conceivable.

It remains an open task to transfer the present results to the MPI context. The extent to which and the conditions under which current MPI models reach their limits of applicability could be further studied using a generalized model that takes the above-mentioned coupling between micromagnetic response and fluid dynamics bidirectionally into account. While the present work considers the causal relationship from fluid dynamics to micromagnetic response only, there is experimental evidence that the other causal direction can become relevant in realistic MPI scenarios [31]. To develop and study such a generalized model is the goal of further studies, which will be based on [32, 33] and literature cited therein.

In addition, experimental studies demonstrating the effects we have shown would be of interest. Preferably such experiments are performed at low excitation frequencies, increased viscosity, and with particles having a large hydrodynamic to core diameter ratio. Performing these in a spectroscopic setup with an additional magnetic gradient field, where Brownian relaxation is dominant [34], would be the most obvious setting. Ultimately, this would also allow to address the question of whether the effect is strong enough to be used for flow measurements or similar applications.

## Acknowledgments

T. Kluth acknowledges funding by the German Research Foundation (DFG, Deutsche Forschungsgemeinschaft) - project 426078691.

## Author's statement

Conflict of interest: Authors state no conflict of interest.

## References

- [1] B. Gleich and J. Weizenecker. Tomographic imaging using the nonlinear response of magnetic particles. *Nature*, 435(7046):1214–1217, 2005.
- [2] M. I. Shliomis. Magnetic fluids. *Soviet Physics Uspekhi*, 17(2):153, 1974.
- [3] R. M. Ferguson, A. P. Khandhar, and K. M. Krishnan. Tracer design for magnetic particle imaging. *Journal of applied physics*, 111(7):07B318, 2012.
- [4] L. M. Bauer, S. F. Situ, M. A. Griswold, and A. C. S. Samia. Magnetic particle imaging tracers: State-of-the-art and future directions. *The journal of physical chemistry letters*, 6(13):2509–2517, 2015.

- [5] H. T. K. Duong, A. Abdibastami, L. Gloag, L. Barrera, J. J. Gooding, and R. Tilley. A guide to the design of magnetic particle imaging tracers for biomedical applications. *Nanoscale*, 2022.
- [6] M. H. Publico-Lansigan, S. F. Situ, and A. C. S. Samia. Magnetic particle imaging: Advancements and perspectives for real-time in vivo monitoring and image-guided therapy. *Nanoscale*, 5(10):4040–4055, 2013.
- [7] R. L. Duschka, J. Haegele, N. Panagiotopoulos, H. Wojtczyk, J. Barkhausen, F. M. Vogt, T. M. Buzug, and K. Lüdtke-Buzug. Fundamentals and potential of magnetic particle imaging. *Current Cardiovascular Imaging Reports*, 6(5):390–398, 2013.
- [8] J. Weizenecker, B. Gleich, J. Rahmer, H. Dahnke, and J. Borgert. Three-dimensional real-time in vivo magnetic particle imaging. *Physics in Medicine & Biology*, 54(5):L1, 2009.
- [9] J. Haegele, J. Rahmer, B. Gleich, J. Borgert, H. Wojtczyk, N. Panagiotopoulos, T. M. Buzug, J. Barkhausen, and F. M. Vogt. Magnetic particle imaging: Visualization of instruments for cardiovascular intervention. *Radiology*, 265(3):933–938, 2012.
- [10] J. Salamon, M. Hofmann, C. Jung, M. G. Kaul, F. Werner, K. Them, R. Reimer, P. Nielsen, A. Vom Scheidt, G. Adam, *et al.* Magnetic particle/magnetic resonance imaging: In-vitro mpi-guided real time catheter tracking and 4d angioplasty using a road map and blood pool tracer approach. *PLoS one*, 11(6):e0156899, 2016.
- [11] S. Herz, P. Vogel, P. Dietrich, T. Kampf, M. A. Rückert, R. Kickuth, V. C. Behr, and T. A. Bley. Magnetic particle imaging guided real-time percutaneous transluminal angioplasty in a phantom model. *Cardiovascular and interventional radiology*, 41(7):1100–1105, 2018.
- [12] P. Ludewig, N. Gdaniec, J. Sedlacik, N. D. Forkert, P. Szwargulski, M. Graeser, G. Adam, M. G. Kaul, K. M. Krishnan, R. M. Ferguson, *et al.* Magnetic particle imaging for real-time perfusion imaging in acute stroke. *ACS nano*, 11(10):10480–10488, 2017.
- [13] M. Gräser, F. Thieben, P. Szwargulski, F. Werner, N. Gdaniec, M. Boberg, F. Griese, M. Möddel, P. Ludewig, D. van de Ven, *et al.* Human-sized magnetic particle imaging for brain applications. *Nature communications*, 10(1):1–9, 2019.
- [14] P. Ludewig, M. Graeser, N. D. Forkert, F. Thieben, J. Rándež-Garbayo, J. Rieckhoff, K. Lessmann, F. Förger, P. Szwargulski, T. Magnus, *et al.* Magnetic particle imaging for assessment of cerebral perfusion and ischemia. *Wiley Interdisciplinary Reviews: Nanomedicine and Nanobiotechnology*, 14(1):e1757, 2022.
- [15] P. Chandrasekharan, Z. W. Tay, D. Hensley, X. Y. Zhou, B. K. Fung, C. Colson, Y. Lu, B. D. Fellows, Q. Huynh, C. Saayujya, *et al.* Using magnetic particle imaging systems to localize and guide magnetic hyperthermia treatment: Tracers, hardware, and future medical applications. *Theranostics*, 10(7):2965, 2020.
- [16] J. Franke, N. Baxan, H. Lehr, U. Heinen, S. Reinartz, J. Schnorr, M. Heidenreich, F. Kiessling, and V. Schulz. Hybrid mpi-mri system for dual-modal in situ cardiovascular assessments of real-time 3d blood flow quantification—a pre-clinical in vivo feasibility investigation. *IEEE Transactions on Medical Imaging*, 39(12):4335–4345, 2020.
- [17] J. Rahmer, J. Weizenecker, B. Gleich, and J. Borgert. Signal encoding in magnetic particle imaging: Properties of the system function. *BMC medical imaging*, 9(1):1–21, 2009.
- [18] P. W. Goodwill and S. M. Conolly. The x-space formulation of the magnetic particle imaging process: 1-d signal, resolution, bandwidth, snr, sar, and magnetostimulation. *IEEE transactions on medical imaging*, 29(11):1851–1859, 2010.
- [19] N. Gdaniec, M. Schlüter, M. Möddel, M. G. Kaul, K. M. Krishnan, A. Schlaefer, and T. Knopp. Detection and compensation of periodic motion in magnetic particle imaging. *IEEE transactions on medical imaging*, 36(7):1511–1521, 2017.
- [20] N. Gdaniec, M. Boberg, M. Möddel, P. Szwargulski, and T. Knopp. Suppression of motion artifacts caused by temporally recurring tracer distributions in multi-patch magnetic particle imaging. *IEEE transactions on medical imaging*, 39(11):3548–3558, 2020.
- [21] C. Brandt and C. Schmidt. Modeling magnetic particle imaging for dynamic tracer distributions. *Sensing and Imaging*, 22(1):1–24, 2021.
- [22] T. Kluth, B. Hahn, and C. Brandt. Spatio-temporal concentration reconstruction using motion priors in magnetic particle imaging, English, in *9th International Workshop on Magnetic Particle Imaging 2019*, T. Knopp and T. M. Buzug, Eds., 23–24, Infinite Science Publishing, 2019.
- [23] J. Ehrhardt, M. Ahlborg, H. Uzunova, T. M. Buzug, and H. Handels. Temporal polyrigid registration for patch-based mpi reconstruction of moving objects. *International Journal on Magnetic Particle Imaging*, 5(1-2), 2019.
- [24] C. Brandt and C. Schmidt. Motion compensation for non-periodic dynamic tracer distributions in multi-patch magnetic particle imaging. *Physics in Medicine & Biology*, 67(8):085005, 2022.
- [25] N. Löwa, P. Radon, O. Kosch, and F. Wiekhorst. Concentration dependent mpi tracer performance. *International Journal on Magnetic Particle Imaging*, 2(1), 2016.
- [26] K. Them. On magnetic dipole–dipole interactions of nanoparticles in magnetic particle imaging. *Physics in Medicine & Biology*, 62(14):5623, 2017.
- [27] D. B. Reeves and J. B. Weaver. Approaches for modeling magnetic nanoparticle dynamics. *Critical Reviews™ in Biomedical Engineering*, 42(1), 2014.
- [28] N.-S. Cheng. Formula for the viscosity of a glycerol- water mixture. *Industrial & engineering chemistry research*, 47(9):3285–3288, 2008.
- [29] R. S. Rosenson, A. McCormick, and E. F. Uretz. Distribution of blood viscosity values and biochemical correlates in healthy adults. *Clinical chemistry*, 42(8):1189–1195, 1996.
- [30] L. Wexler, D. H. Bergel, I. T. Gabe, G. S. MAKIN, and C. J. MILLS. Velocity of blood flow in normal human venae cavae. *Circulation Research*, 23(3):349–359, 1968.
- [31] F. Griese, P. Ludewig, C. Gruettner, F. Thieben, K. Müller, and T. Knopp. Quasi-simultaneous magnetic particle imaging and navigation of nanomag/synomag-d particles in bifurcation flow experiments. *International Journal on Magnetic Particle Imaging*, 6(2 Suppl 1), 2020.
- [32] H. Garcke, P. Knopf, S. Mitra, and A. Schlömerkemper. Strong well-posedness, stability and optimal control theory for a mathematical model for magneto-viscoelastic fluids. *Calculus of Variations and Partial Differential Equations*, 61:179, 2022.
- [33] S. Mitra and A. Schlömerkemper. Magnetoviscoelastic models in the context of magnetic particle imaging. *International Journal on Magnetic Particle Imaging*, 8(1 Suppl 1), 2022.
- [34] J. B. Weaver, A. M. Rauwerdink, C. R. Sullivan, and I. Baker. Frequency distribution of the nanoparticle magnetization in the presence of a static as well as a harmonic magnetic field. *Medical physics*, 35(5):1988–1994, 2008.